

Cite this: *Chem. Commun.*, 2011, **47**, 2670–2672

www.rsc.org/chemcomm

Quininium mandelates—a systematic study of chiral discrimination in crystals of diastereomeric salts†

Nikoletta B. Báthori,^{*a} Luigi R. Nassimbeni^a and Clive L. Oliver^b

Received 7th October 2010, Accepted 10th December 2010

DOI: 10.1039/c0cc04279j

The selectivity profile for the resolution of mandelic acid by quinine is dominated by structures comprising (QUIN⁺)-(MAND⁻) salts with $Z' = 3$ which contain (*R*)-, (*R*)- and (*S*)-mandelate anions.

The resolution of racemic modifications by a chiral resolving agent is generally achieved either by diastereomer salt formation or by inclusion with a chiral host compound. The former method is the most common, and has been reviewed.¹

The cinchona alkaloids, of which quinine is the most abundant, have been used extensively as resolving agents for acids^{1,2} and the pairs quinine/quinidine and cinchonidine/cinchonine have been described as “quasi-enantiomeric”.³ Larsen^{4,5} has described the structures of the salts formed by cinchonine and cinchonidine with both (*R*)- and (*S*)-mandelic acids. She concluded that cinchoninium (*R*)-mandelate is the less soluble salt and its structure displays disorder in the $-\text{CH}=\text{CH}_2$ moiety. In contrast, cinchonidinium-(*S*)-mandelate is the less soluble salt. The thermal and solubility parameters of the four salts were reconciled with their crystal structures and it was noted that the packing of the cinchonidinium salts was significantly different from their corresponding cinchoninium salts.

We have taken a somewhat different approach to the question of enantiomeric resolution in order to understand the mechanism of the molecular recognition that drives the differentiation of the resolving agent for one particular enantiomer. We have thus set up a series of competition experiments where the resolving agent, quinine (QUIN) was exposed to mixtures of mandelic acid, where the mole fraction of the starting mixture was varied systematically. The ensuing solutions were allowed to crystallise and the mole fraction of the entrapped enantiomer was measured by analysing the crystal structure. This is an extension of the technique employed to measure the selectivity profile of a given host

compound (H) towards a pair of guests A and B, whereby H is dissolved in a series of solutions where the mole fraction X_A varies in steps from 0 to 1. The resulting crystals are analysed, yielding mole fractions of A as Z_A . The selectivity coefficient at each point is then defined as

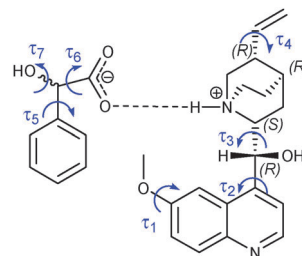
$$K_{A:B} = (K_{B:A})^{-1} = Z_A/Z_B \times X_B/X_A; (X_A + X_B = 1)$$

and is a measure of the discrimination of the host for a given guest. In our case the two guests are replaced by (*R*)- and (*S*)-mandelic acids.

The crystals were grown by slow evaporation from solution containing 1 mmol of quinine (QUIN) and 1 mmol of mandelic acid (MAND) in 20 mL of ethanol. The mole fraction of the (*R*)-mandelic acid in the starting solution was varied systematically as X_R (%) = 15, 30, 70 and 100. The crystals were analysed by X-ray diffraction and the crystallographic data are summarised in the ESI† in Table 1S.‡ Refinement revealed that all structures are salts of quininium cations and mandelate anions (Scheme 1). In all cases we checked that the structure of the single crystals was representative of the bulk by measuring the X-ray powder patterns.

The (QUIN⁺)(15*R*-MAND⁻) structure (**1**) crystallises in $P2_12_12_1$ with $Z' = 1$ and only the (*S*)-mandelate ion was captured, and is essentially the same as that published by Gjerlov and Larsen⁶ (data at 122 K). However, our data were collected at 173 K because prior data collections for the other structures in this study were performed at this temperature. The metrics of the hydrogen bonds for this and the subsequent structures are reported in Table 2S.†

The (QUIN⁺)(30*R*-MAND⁻) structure (**2**) crystallises in the space group $P2_1$ with $Z' = 3$. There are thus three pairs of ions in the asymmetric unit. The (QUIN⁺)(MAND⁻) ion pairs are labelled A, B and C, and the configurations of the



Scheme 1

^a Centre for Crystal Engineering, Department of Chemistry, Cape Peninsula University of Technology, P.O. Box 652, Cape Town, 8000, South Africa. E-mail: bathorin@cput.ac.za; Fax: +27 21 460 3854; Tel: +27 21 460 8354

^b Centre for Supramolecular Chemistry Research, Department of Chemistry, University of Cape Town, South Africa

† Electronic supplementary information (ESI) available: X-Ray data collection and structure refinement details,⁹ crystallographic information of structures **1**–**5**, hydrogen bond parameters, torsion angles. CCDC 795245–795249. For ESI and crystallographic data in CIF or other electronic format see DOI: 10.1039/c0cc04279j

mandelate anions are (*R*), (*R*) and (*S*), respectively. The mole fraction of the (*R*)-mandelate in this crystal is thus Z_R (%) = 67.

The (QUIN⁺)(50*R*-MAND⁻) structure (**3**) is similar to structure **2** in that it has comparable unit cell parameters and $Z' = 3$. However the 'C' mandelate ion is partly disordered, and careful refinement showed that both (*R*) and (*S*) anions are located on this site, with occupancies of 18% and 82%, respectively. The overall mole fraction Z_R for this structure is therefore 72.6%. An analogous situation is exhibited by the (QUIN⁺)(70*R*-MAND⁻) structure (**4**), yielding $Z_R = 77.0\%$.

We had considerable difficulties in growing suitable crystals of the (QUIN⁺)(100*R*-MAND⁻) salt (**5**). Using pure ethanol as the solvent and varying the initial concentrations and cooling conditions yielded poor quality crystals with large mosaic spreads. We repeated the crystallisation in a variety of solvents, namely methanol, acetonitrile, ethylacetate, dichloromethane, acetone, iso-propanol, benzene, methyl-ethylketone and 1 : 1 (v/v) water mixtures of these when possible. More than thirty different crystallisations were attempted. The optimal results were obtained with an ethanol/water mixture (v/v = 5 : 1). The crystal which we eventually employed had high mosaic spread and was subjected to a long intensity data collection. (For details see ESI.†) The resulting structure is similar to the previous three, in that it crystallises in $P2_1$ with $Z' = 3$.

The selectivity diagram for the quinine–mandelic acid system is shown in Fig. 1. Structure **1** contains only the (*S*)-enantiomer of the mandelate anion. Structures **2–5** are similar, in that they all crystallise in the space group $P2_1$ with $Z' = 3$, have similar unit cell dimensions and contain Z_R varying from 0.67–1. Each salt pair stabilised by (QUIN)N⁺–H···OOC(MAND) hydrogen bonds with N···O distances varying from 2.56–2.79 Å.

We may regard structure **2** as representative of structures **3** and **4** as they all contain the (*R*)-, (*R*)- and (*S*)-mandelate anions on the same site. It is therefore instructive to compare structure **2** with structure **5** which contains only (*R*)-mandelates. The packing of these two structures is shown in Fig. 2 and is characterized by hydrogen bonded chains running along [101].

In order to understand the mechanism of enantiomeric resolution we analysed the torsion angle changes which occurred in the host cation and guest anion as the composition Z_R changed. We recorded the torsion angles τ_1 – τ_4 (QUIN⁺) and τ_6 – τ_7 (MAND⁻) (Scheme 1). These are summarised in Table S3.† We noted that τ_1 , τ_2 , τ_3 and τ_6 remained essentially constant for all structures, while τ_4 takes a value of $\sim 180^\circ$ for cation A and $\sim -110^\circ$ for cations B and C. The only

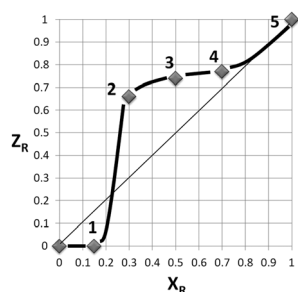


Fig. 1 Selectivity curve of the quinium–mandelate system.

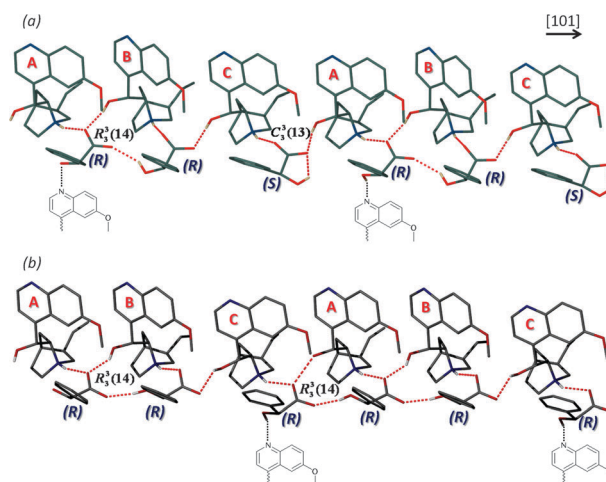


Fig. 2 Hydrogen bonds between salt pairs in structures **2** and **5**.

significant changes in the anions occurred in τ_5 when the configuration changed from *R* to *S* and in τ_7 which is controlled by the hydrogen bonding of the hydroxyl moiety.

Fig. 2a displays six salt pairs of structure **2**, each labelled A, B and C. We note a ring system of hydrogen bonds between moieties A and B which may be described as $R_3^3(14)$.⁷ This is repeated in structure **5**, shown in Fig. 2b. The important difference in the two structures occurs in moieties C. In structure **2** the (*S*)-mandelate displays an intramolecular –OH···O bond and there is a chain of single hydrogen bonds joining (MAND⁻_B)···(QUIN⁺_C)···(MAND⁻_C)···(QUIN⁺_A) symbolised as $C_3^3(13)$. In contrast, in structure **5** anion C does not show an intramolecular H-bond, but gives rise to a second ring system $R_3^3(14)$ and in addition is stabilised by the hydroxo-moiety bonding to a neighbouring (QUIN⁺) via an –OH···N bond.

The selectivity curve displayed in Fig. 1 shows that there is a large range of stability in the structures formed from $X_R \approx 22\%$ to 85% (structures **2**, **3** and **4**). Each of these crystallises in $P2_1$ with $Z' = 3$ and, essentially, captures two (*R*)- and one (*S*)-mandelate anions. Thus it is important to understand the essential differences between these three structures and that of structure **5** which crystallised with all three (*R*)-mandelates.

In order to comprehend the difference in the packing forces which stabilise the structures, we have carried out an analysis of the non-bonding interactions in structure **2** (representative of structures **3** and **4** as well) and compared this to the results of structures **1** and **5**. We thus employed the program Crystal Explorer⁸ to generate the related fingerprint plots of the salt pairs instead of the individual molecules in the structures (Fig. 3). The fingerprint plots reflect the non-bonding interactions between neighbouring salt pairs and therefore do not show the (QUIN)–N⁺–H···OOC(MAND) hydrogen bond occurring within each pair. However, they give an overview of the supramolecular packing of the crystal. Fig. 3a is a representation of all the interactions in structure **1**. Peaks ① and ② arise from intermolecular (QUIN⁺)–OH···OOC(MAND) hydrogen bonds and peak ③ represents the H···H contacts. An important feature is the spread of the latter interactions which occur at $d_i = d_c > 2.4$ Å. This is a feature of a loosely packed structure, which is reflected in this low density of 1.203 g cm⁻³ and high

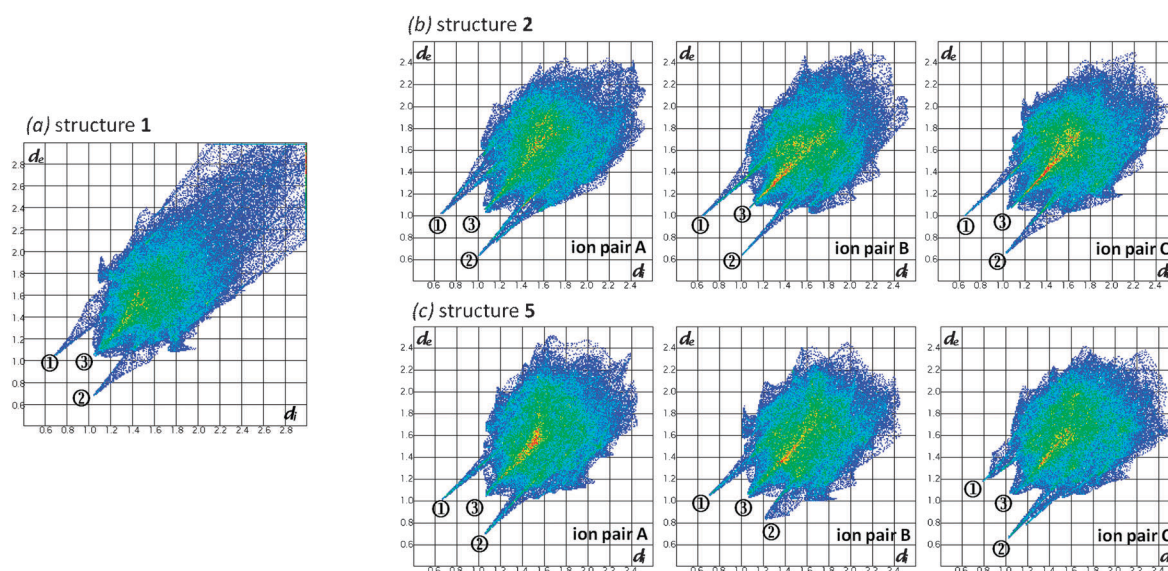


Fig. 3 Fingerprint plots of ion pairs in structures 1, 2 and 5.

value of the volume/non-hydrogen atom of 18.79 \AA^3 . In contrast structures 2 to 5 are packed more efficiently and have densities varying from 1.316 to 1.340 g cm^{-3} and corresponding volume/non-H atom varying from 17.17 to 16.87 \AA^3 . Fig. 3b and c shows the fingerprint plot for the salt pairs A, B and C of structures 2 and 5. The plots for the A pairs are similar but we note significant differences in the plots for the B and C pairs. In particular peaks ① and ② of the B and C pairs of structure 2 arise from $(\text{QUIN}^+) \text{--OH} \cdots \text{OOC}(\text{MAND})$ hydrogen bonds. These are strong interactions in which the $\text{H} \cdots \text{O}$ distances are $\sim 1.65 \text{ \AA}$. The corresponding peaks in structure 5 are different, in that for salt pair B, peak ① due to a $(\text{QUIN}^+) \text{--OH} \cdots \text{OOC}(\text{MAND})$ interaction is weaker with $\text{H} \cdots \text{O} \approx 1.77 \text{ \AA}$ and peak ② is weaker, more diffuse and is due to a bifurcated $(\text{QUIN}^+) \text{--OH} \cdots \text{OOC}(\text{MAND})$ hydrogen bond. In structure 5, pair C, we note a diffuse peak ① due to a weak $(\text{QUIN}^+) \text{--OH} \cdots \text{OOC}(\text{MAND})$ interaction and a peak ② which arises from two distinct interactions, namely $(\text{QUIN}) \text{--OH} \cdots \text{OOC}(\text{MAND})$ and $(\text{MAND}^-) \text{--OH} \cdots \text{N}(\text{QUIN}^+)$ hydrogen bond, both being weak interactions. This shows that there are stronger intermolecular forces stabilising structure 2 in comparison with those of structure 5. We propose that these are the forces responsible for the greater stability of structure 2 and this explains the mechanism of resolution, whereby the structures with [(R), (R), (S)-mandelates] are obtained over a large range of the selectivity profile.

We conclude that the resolution of mandelic acid by quinine is driven by intermolecular hydrogen bonds and concomitant changes in some torsion angles of the (QUIN^+) and (MAND^-) ions. These give rise to stable structures of three salt pairs in the crystallographic asymmetric unit containing (R)-, (R)- and (S)-mandelate anions, and dominate a large range of the selectivity profile.

Notes and references

† Crystal data for 1: $\text{C}_{28}\text{H}_{32}\text{N}_2\text{O}_5$, $M = 476.56$, orthorhombic, $P2_12_12_1$, $a = 22.5852(4) \text{ \AA}$, $b = 22.5852(4) \text{ \AA}$, $c = 7.5192(3) \text{ \AA}$, $\alpha = \beta = \gamma = 90^\circ$, $V = 2630.7(13) \text{ \AA}^3$, $T = 173(2) \text{ K}$, $Z = 4$, 3704 out of 4832 with $I > 2s(I)$, $R_1 = 0.0514$ ($I > 2\sigma(I)$), $wR_2 = 0.1316$ (all data). Crystal data for 2:

$\text{C}_{28}\text{H}_{32}\text{N}_2\text{O}_5$, $M = 476.56$, monoclinic, $P2_1$, $a = 10.4121(14) \text{ \AA}$, $b = 18.574(3) \text{ \AA}$, $c = 19.070(3) \text{ \AA}$, $\beta = 102.635(3)^\circ$, $V = 3598.6(8) \text{ \AA}^3$, $T = 173(2) \text{ K}$, $Z = 6$, 12026 out of 19779 with $I > 2s(I)$, $R_1 = 0.0461$ ($I > 2\sigma(I)$), $wR_2 = 0.1273$ (all data). Crystal data for 3: $\text{C}_{28}\text{H}_{32}\text{N}_2\text{O}_5$, $M = 476.56$, monoclinic, $P2_1$, $a = 10.381(3) \text{ \AA}$, $b = 18.456(5) \text{ \AA}$, $c = 19.036(5) \text{ \AA}$, $\beta = 102.557(5)^\circ$, $V = 3559.7(18) \text{ \AA}^3$, $T = 173(2) \text{ K}$, $Z = 6$, 12252 out of 42152 with $I > 2s(I)$, $R_1 = 0.0519$ ($I > 2\sigma(I)$), $wR_2 = 0.1239$ (all data). Crystal data for 4: $\text{C}_{28}\text{H}_{32}\text{N}_2\text{O}_5$, $M = 476.56$, monoclinic, $P2_1$, $a = 10.4377(14) \text{ \AA}$, $b = 18.501(2) \text{ \AA}$, $c = 19.116(2) \text{ \AA}$, $\beta = 102.318(2)^\circ$, $V = 3606.5(8) \text{ \AA}^3$, $T = 173(2) \text{ K}$, $Z = 6$, 11667 out of 47197 with $I > 2s(I)$, $R_1 = 0.0362$ ($I > 2\sigma(I)$), $wR_2 = 0.0855$ (all data). Crystal data for 5: $\text{C}_{28}\text{H}_{32}\text{N}_2\text{O}_5$, $M = 476.56$, monoclinic, $P2_1$, $a = 10.415(2) \text{ \AA}$, $b = 18.416(4) \text{ \AA}$, $c = 18.845(4) \text{ \AA}$, $\beta = 101.431(7)^\circ$, $V = 3542.8(14) \text{ \AA}^3$, $T = 173(2) \text{ K}$, $Z = 6$, 12740 out of 28583 with $I > 2s(I)$, $R_1 = 0.0556$ ($I > 2\sigma(I)$), $wR_2 = 0.1437$ (all data). CCDC 795245–795249.

- 1 Optical resolution via diastereomeric salt formation, ed. D. Kozma, CRC Press, New York, 2002.
- 2 (a) S. H. Wilen and E. L. Eliel, *Tables of resolving agents and optical resolution*, Univ. of Notre Dame Press, Notre Dame London, 1971; (b) J. Jacques, A. Collet and S. H. Wilen, *Enantiomers, Racemates and Resolutions*, Krieger Publishing Company, Malabar, Florida, 1994.
- 3 R. B. Woodward, P. M. Cava, W. D. Ollis, A. Hunger, H. U. Daeniker and K. Schenker, *Tetrahedron*, 1963, **19**, 247.
- 4 S. Larsen, H. Lopez de Diego and D. Kozma, *Acta Crystallogr., Sect. B: Struct. Sci.*, 1993, **49**, 310–316.
- 5 A. Gjerlov and S. Larsen, *Acta Crystallogr., Sect. B: Struct. Sci.*, 1997, **53**, 708–718.
- 6 A. Gjerlov and S. Larsen, *Acta Crystallogr., Sect. C: Cryst. Struct. Commun.*, 1997, **53**, 1505–1508.
- 7 S. Eppel and J. Bernstein, *Acta Crystallogr., Sect. B: Struct. Sci.*, 2008, **64**, 50–56.
- 8 (a) J. J. McKinnon, M. A. Spackman and A. S. Mitchell, *Acta Crystallogr., Sect. B: Struct. Sci.*, 2004, **60**, 627; (b) M. A. Spackman and J. J. McKinnon, *CrystEngComm*, 2002, **4**, 378.
- 9 Bruker APEX2. Version 1.0–27., Bruker AXS Inc., Madison, Wisconsin, USA, 2005; Z. Otwinowski and W. Minor, in *International Tables for Crystallography, Vol. F*, ed. M. G. Rossmann and E. Arnold, Kluwer, Dordrecht, 2000; Bruker, SAINT-Plus (including XPREP). Version 7.12., Bruker AXS Inc., Madison, Wisconsin, USA, 2004; Bruker, XPREP2. Version 6.14., Bruker AXS Inc., Madison, Wisconsin, USA, 2003; G. M. Sheldrick, *SHELXS-97 and SHELXL-97 Programs for crystal structure determination and refinement*, University of Göttingen, 1997; L. J. Barbour, *J. Supramol. Chem.*, 2001, **1**, 189–191; A. L. Spek, *PLATON, A Multipurpose Crystallographic Tool*, Utrecht University, Utrecht, The Netherlands, 2008; G. M. Sheldrick, *CELL_NOW Version 2008-2, Index Twins and Other Problem Crystals*, University of Göttingen, 2008.